Electronic Supplementary Material (ESI) for ChemComm.

Supplementary Information

Highly efficient electrocatalyst based on double perovskite cobaltites with immense intrinsic catalytic activity for water oxidation

Håkon Andersen,[a] Kaiqi Xu,[a] Dmitry Malyshkin,[b,c] Ragnar Strandbakke,[a*] Athanasios Chatzitakis[a*]

[a] Centre for Materials Science and Nanotechnology, Department of Chemistry, University of Oslo, FERMiO, Gaustadalléen 21, NO-0349 Oslo, Norway

[b] Department of Physical and Inorganic Chemistry, Institute of Natural Sciences and Mathematics, Ural Federal University, Ekaterinburg, 620000, Russia

[c] Institute of High Temperature Electrochemistry, 620137 Ekaterinburg, Russia

Experimental details

Synthesis of electrode powders

Powder samples of nominal compositions $BaGdCo_{1.8}Fe_{0.2}O_{6-\delta}$, $BaPrCo_2O_{6-\delta}$ and $BaPrCo_{1.4}Fe_{0.6}O_{6-\delta}$ were prepared by means of a glycerol nitrate method using Gd_2O_3, Pr_6O_{11}, $La(NO_3)_3{\cdot}6H_2O$ (ZAO Lanhit), $BaCO_3$, Co_3O_4, $FeC_2O_4{\cdot}2H_2O$ (ZAO Vekton) as starting materials. All materials used had specified purities of 99.99%. Stoichiometric mixtures of the starting materials were dissolved in concentrated nitric acid (99.99% purity), and the required volume of glycerol (99% purity) was added as complexing agent and fuel. The glycerol quantity was calculated according to full reduction of corresponding nitrates to molecular nitrogen, N_2. The as-prepared solutions were heated at 100°C until water had evaporated, whereupon the dried product pyrolysed. The resulting ash was calcined at 1100°C for 10 hours to obtain the double perovskite powder. The phase composition of the powder was confirmed by X-ray diffraction (XRD) with an Equinox 3000 diffractometer (Inel, France) using Cu K_α radiation. XRD showed no indications of second phases in the as-prepared samples (Figure S1).

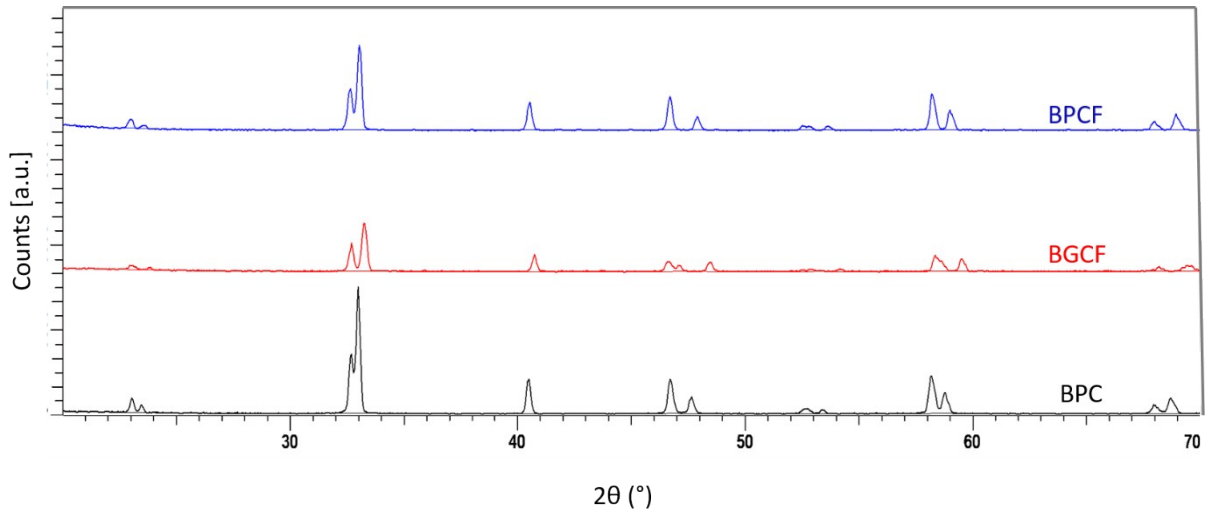

Figure S1: XRD of as-prepared BPCF, BGCF and BPC powders.

Hydrogen evolution reaction

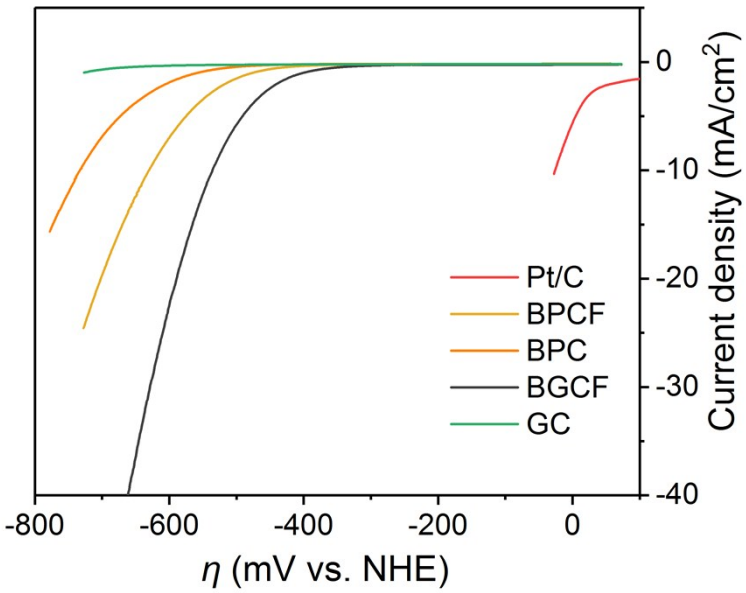

Figure S2: LSV curves of the double perovskites, Pt/C (10% Pt loading on Vulcan carbon black) and bare GC. The potential scanning rate was 10 mV/s in 1 M NaOH.

Faradaic Efficiency

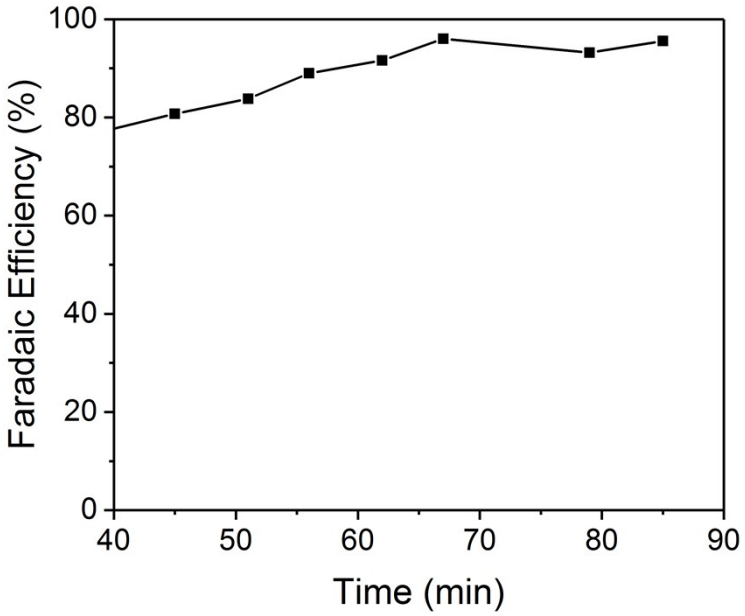

Figure S3: Faradaic efficiency of BGCF at 10 mA/cm^2 in 1 M NaOH, in a two-electrode configuration with Pt as the cathode.

The O_2 gas was measured with an Agilent 3000A Micro GC and the gas samples were collected automatically from a 60 ml headspace. The values presented in Figure S3 are a bit underestimated as the Micro GC samples approx. 3 ml each time that are compensated by an Ar overpressure line. Ar gas was used to remove the dissolved O_2 gas from the solution, as well as the air in the headspace. It is also known that there is an hysteresis in the Faradaic efficiency during the initiation of the electrolysis, that is why the first 40 min are omitted from the graph. Another reason is that the injection line is approx. 1 m long, hence the concentration measured by the GC may not instantly represent the concentration in the headspace. Moreover, the hysteresis is also due to the relatively low nominal surface of the electrode (1 cm^2) compared to the headspace and total value of the sealed electrolysis cell (138 ml).

Stability

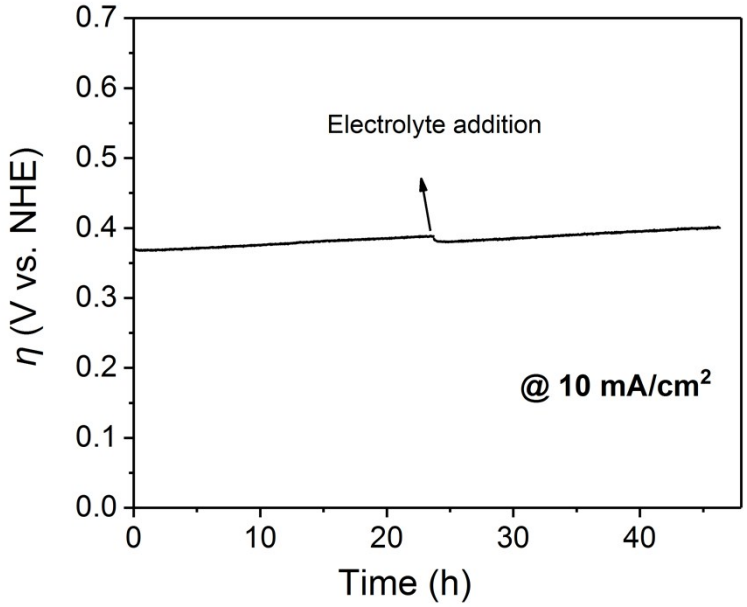

Figure S4: Galvanostatic experiments at a current density of 10 mA/cm^2 in 1 M NaOH for 48 h and Hg/HgO (1M NaOH) as the reference electrode.

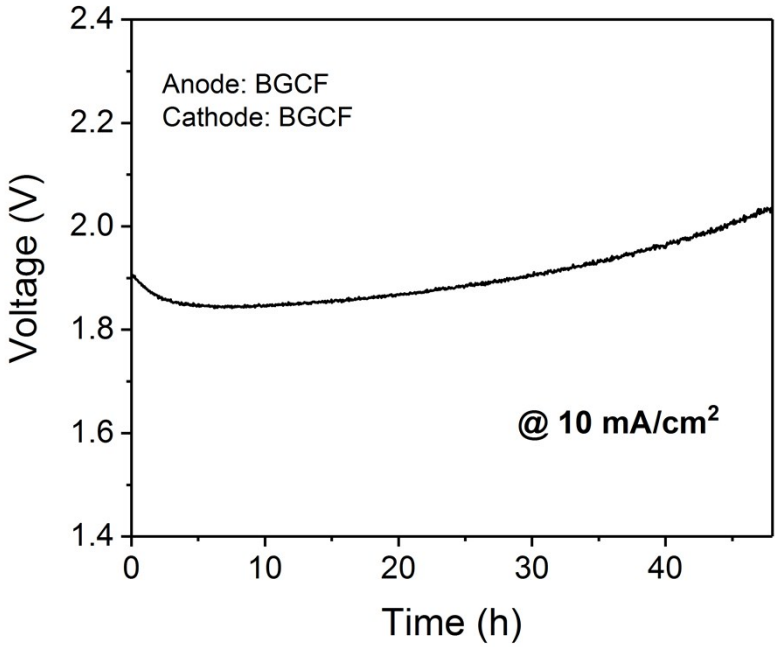

Figure S5: Galvanostatic experiments at a current density of 10 mA/cm^2 in 1 M NaOH for 48 h in a two-electrode configuration with BGCF as both the anode and cathode electrocatalyst.

Electroactive surface area

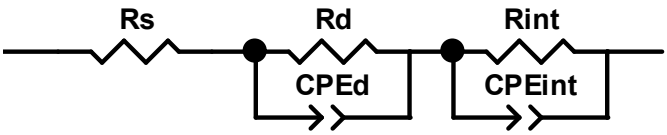

Figure S6: Equivalent circuit (EQC) used to fit the raw EIS data. All fittings were performed in Zview and all chi-square values were of the order of 10^{-4}. R_s accounts for the solution resistance. R_d and CPE_d account for the resistance and constant phase element for the diffusion/migration of ionic species in porous electrodes, respectively. This simplified approach is proposed instead of the transmission line model.[1, 2] R_{int} and CPE_{int} are assigned as the interfacial charge transfer resistance and constant phase elements respectively. Using this approach as $R_{ct} = R_d + R_{int}$ and after the CPEs are transformed into capacitances (see explanation in Fig. 4 in the main document), $C_{dl} = \frac{1}{\frac{1}{C_d} + \frac{1}{C_{int}}}$. It should be noted that a simple Randles circuit gave poor deconvolutions and it was found inappropriate.

Table S1: Comparison between capacitance values as obtained by cyclic voltammetry at the potential range 1.0-1.1 V vs. NHE, and capacitance values as extracted by EIS at two potential regions. $R_{ct}C_{dl}$ parameter

Catalyst	**Capacitance from CV scanning (μF/cm²)**	**Capacitance from EIS at 1.09 mV vs. NHE (capacitive region) (μF/cm²)**	**Capacitance at 10 mA/cm² (OER region) (μF/cm²)**	**$R_{ct}C_{dl}$ – τ (s) at 10 mV overpotential (capacitive region)**
IrO_2	623	361	1550	**7.39**
BGCF	102	69	68	1.03
BPCF	136	161	61	0.71
BPC	344	287	297	2.05

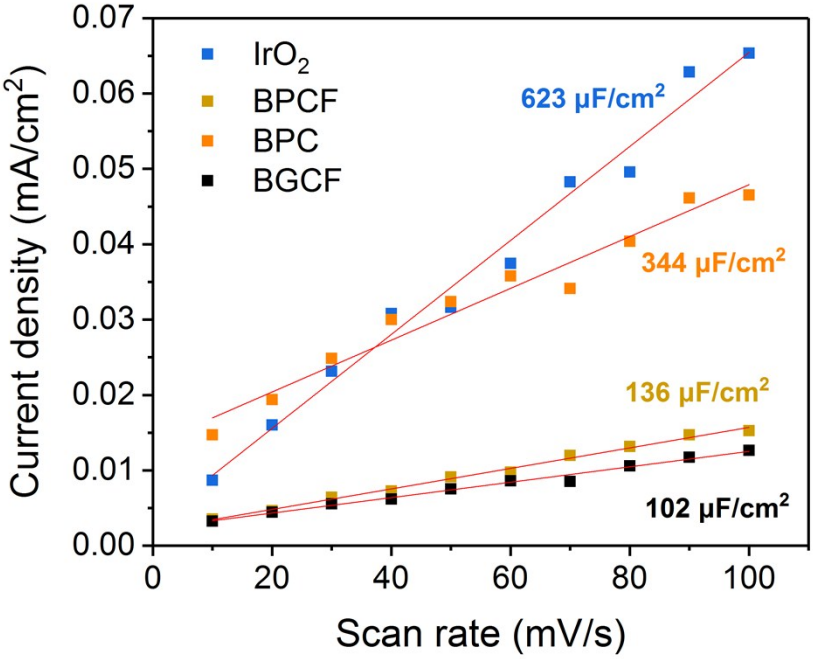

Figure S7: Double layer capacitances as extracted by CV measurements at different scanning rates. The CV was performed in the capacitive area and in the range of 1.0-1.1 V vs. NHE.

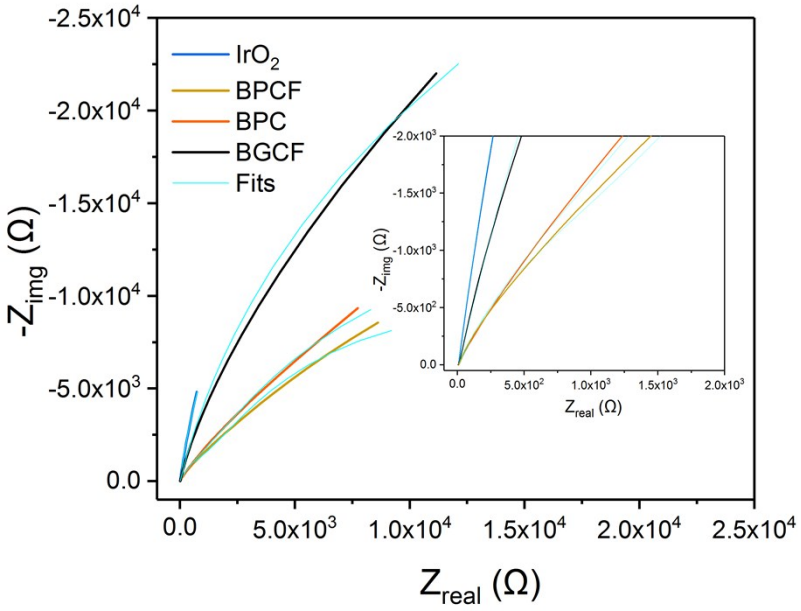

Figure S8: Nyquist plots recorded in the frequency range from 100 kHz to 1 Hz with an imposed sinusoidal voltage of 10 mV. The EIS measurements were performed at the capacitive region at a DC potential of 1.09 V vs. NHE.

Scanning Electron Microscopy (SEM)

The microstructure of the as-prepared powders was examined by SEM and compared with the IrO_2 powder, which was used as the reference electrocatalyst.

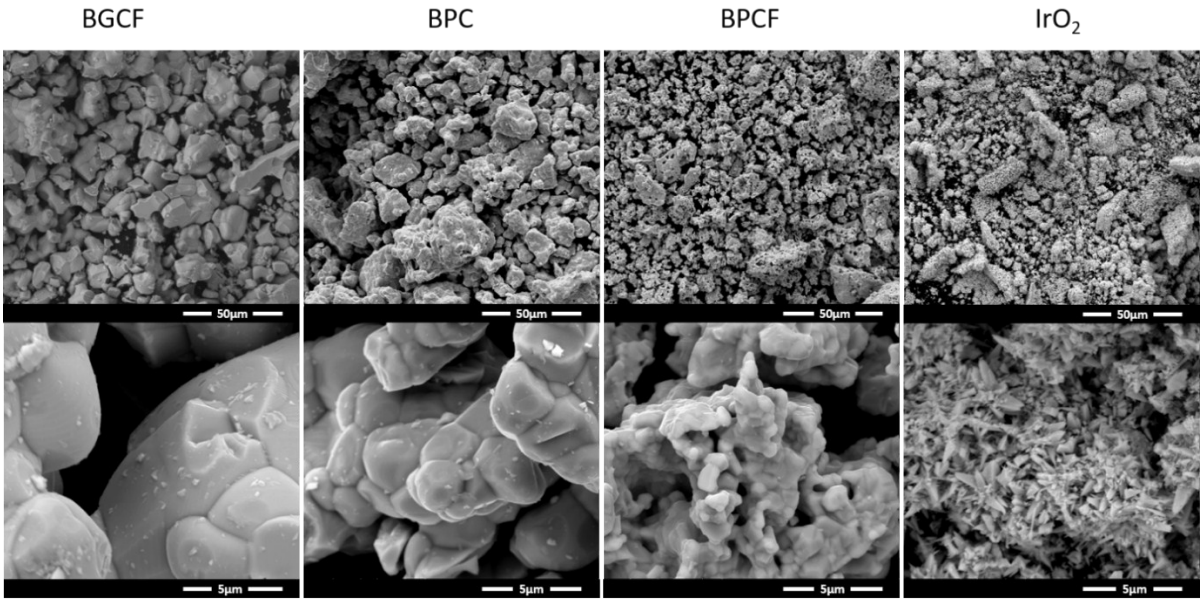

Figure S9: SEM micrographs of BGCF, BPC, BPCF and IrO_2 powders used as EC on glassy carbon and Ni foam electrodes.

References

1. A. Papaderakis, N. Pliatsikas, P. Patsalas, D. Tsiplakides, S. Balomenou, A. Touni and S. Sotiropoulos, *Journal of Electroanalytical Chemistry*, 2018, **808**, 21-27.
2. L. Birry and A. Lasia, *Journal of Applied Electrochemistry*, 2004, **34**, 735-749.